ENERGY-FLUX BALANCES AND SOURCE TERM PARAMETERIZATIONS

[1,3]Will Perrie, [2]Don Resio and [3]Adhi Susilo

[1]Fisheries & Oceans Canada, BIO, Dartmouth, Nova Scotia, Canada
[2] ERDC-Coastal and Hydraulics Lab, USA
[3]Dalhousie Univ., Halifax, NS., Canada

1. INTRODUCTION

Source terms within wave models are often tested in terms of parametric balance: their ability to satisfy specified relationships among dimensionless energy and fetch variables (Komen et al., 1984; WAMDI, 1988). While compliance of wave models to these basic conditions is essential for all applications, further requirements, including detailed spectral balance, are necessary to move beyond current parameterizations for source terms, and address model inadequacies in operational models. The motivation for this paper is recently collected data and the concomitant new wave insights that have developed relating to detailed balance. These new insights are concerned with the development of the observed spectral wave equilibrium range and its maintenance by source terms for wind input energy S_{in}, wave dissipation S_{ds} and nonlinear wave-wave interactions S_{nl}, as formulated in widely used state-of-the-art operational wave models (WAM, SWAN and WaveWatch). Up to this point, studies trying to optimize formulations for wind input S_{in} and dissipation S_{ds} in relation to nonlinear interactions S_{nl} have been hampered by the large number of degrees of freedom within the wave spectra. This has led to the need to highly parameterize S_{nl}, as is evident in the discrete interaction approximation DIA, implemented in WAM-type models.

In this manuscript, we identify selected problem areas in present operational models, in regard to source terms (S_{nl}, S_{in}, and S_{ds}). This discussion includes consideration of their representation of the equilibrium range, and also Phillips' α coefficient. At the Workshop, we will present results concerning constraints on S_{in}, and S_{ds}, related to a modern version of the RTW (Resio – Tracy –Webb) S_{nl} formulation (Tracy and Resio 1982; Resio and Perrie, 1991). This is based on a revised formulation of the RTW algorithm.

2. DIA COMPARED TO 'EXACT' RESULTS

DIA represents the nonlinear interactions S_{nl} by a 2-dimensional integration involving two discrete interactions (Komen et al., 1994) defined by

$$\omega_1 = \omega_2 = \omega \quad (1)$$

$$\omega_3 = \omega(1+\lambda) \quad (2)$$

$$\omega_4 = \omega(1-\lambda) \quad (3)$$

where $\lambda = 0.25$ and the resonance conditions imply angles for $\mathbf{k}_3$ and $\mathbf{k}_4$, respectively $\theta_3 = 11.5^o$ and $\theta_4 = -33.6^o$. This is in place of the full Boltzmann representation for wave-wave interactions, involving a 6-dimensional integration, which is effectively reduced to 3 dimensions by the resonance conditions (Tracy, 1982; Webb, 1978). An example of the loci of interactions for DIA compared to those for the full Boltzmann representation of the nonlinear interactions S_{nl}, as simulated by the revised RTW formulation of S_{nl}, is given in Figs. 1a-1b.

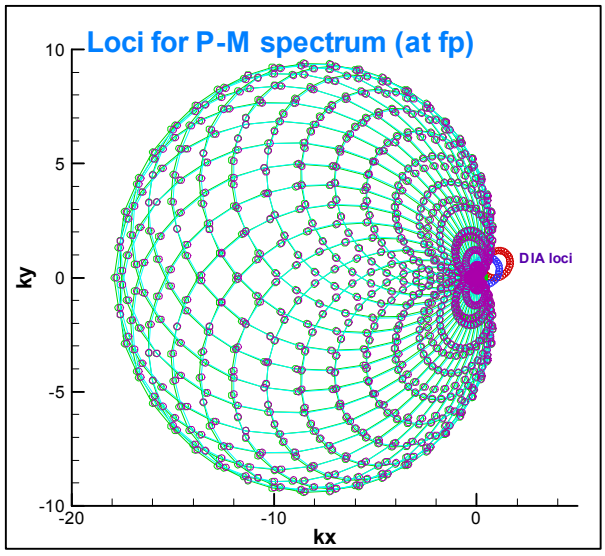

Figure 1a. Loci of interactions for RTW formulation of S_{nl} compared to that of DIA, assuming a Pierson – Moskowitz (P-M) spectrum. One of the interacting 4-waves is fixed at the spectral peak f_p.

This computation assumes a Pierson-Moskowitz wave spectrum. The complexity of the loci available to the RTW formulation of S_{nl} in comparison to that of DIA is

striking. A similar comparison is possible comparing the coupling coefficient in the RTW formulation to the simple constant used by DIA.

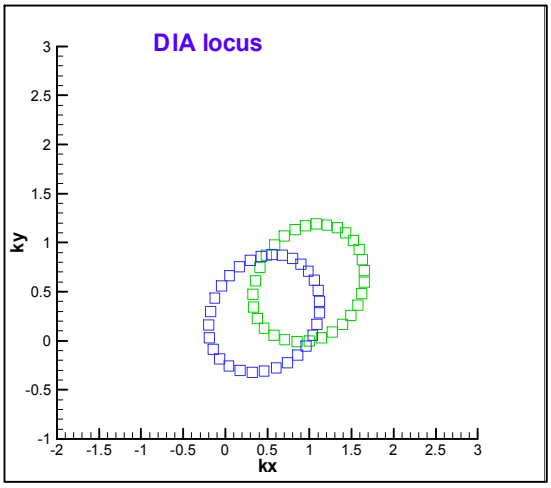

Figure 1b. As in Figure 1a, loci for vectors $\mathbf{k}_2$ and $\mathbf{k}_4$ in the DIA formulation.

The original comparison of the DIA to an exact integral form for nonlinear interactions was presented by Hasselmann et al. (1985). See also Komen et al. (1994). This comparison represented an "optimal" tuning of the DIA for the case of a standard JONSWAP spectrum. For model estimates of significant wave height Hs, the DIA formulation is an acceptable approximation. Moreover, for 1-dimensional estimates of nonlinear transfer S_{nl} and spectral wave energy, DIA is still acceptable (Fig. 3.6, Koman et al., 1994),

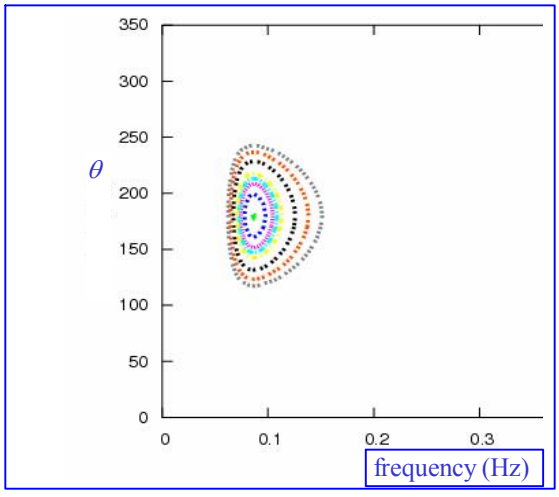

Fig. 2a. Input energy spectrum $E(f,\theta)$ as a function of frequency f, and direction θ.

compared with full-Boltzmann representations of the nonlinear interactions S_{nl}. Certainly DIA computations are very economical compared to RTW computations.

However, it is known that for 2-dimensional representations of spectral wave energy $E(f,\theta)$, DIA estimates can be far from those generated by the more complete representation of the nonlinear interactions. Resio et al. (1992) showed that comparisons for more peaked and /or more complicated spectra produced comparisons that were substantially degraded from the tuned comparison. In particular they showed that, in situations with strong variations of mean wave angle as a function of frequency, the DIA formulation missed most of the magnitudes and the major features of the full-integral representation for S_{nl}.

In Fig. 2a-2d we present a simple spectral form for $E(f,\theta)$ with (f_p=0.1, α = 0.01, γ = 1), comparing the DIA results for S_{nl} with 'exact' results: (1) namely an earlier version of the Resio-Tracy-Webb (RTW) algorithm formulated in the current version of the operation WaveWatchIII (hereafter RTW-ww3) NCEP wave model, and (2) a new revised RTW formulation as recently developed at the ERDC Coastal and Hydraulics Lab (hereafter RTW-erdc).

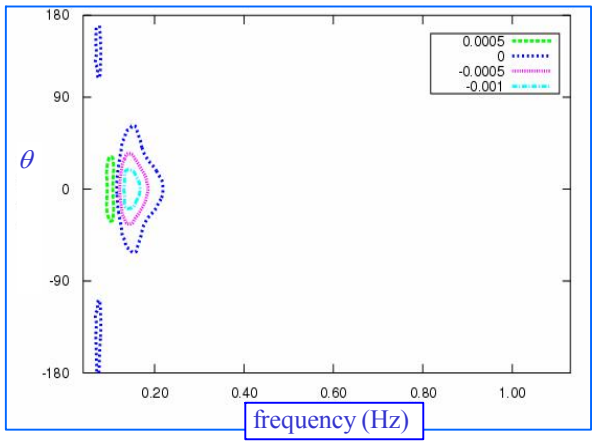

Fig. 2b. Nonlinear transfers S_{nl} for $E(f,\theta)$ from Fig. 2a, using DIA formulation from WW3.

It is clear that distortion is present in DIA, compared to either the old or the new improved version of RTW. A notable feature in the RTW-erdc result in Figure 2d is the presence of equilibrium range nonlinear transfers which are not so evident in either the DIA result in Fig. 2b, or the RTW-ww3 results in Fig. 2c. This is of interest within the context of the "null point" f_o (discussed later). Figure 2d also suggests that a stronger transfer to the forward face and equilibrium range results from RTW-erdc, than from either DIA or RTW-ww3. This could be of importance for satisfying detailed and parametric balance conditions.

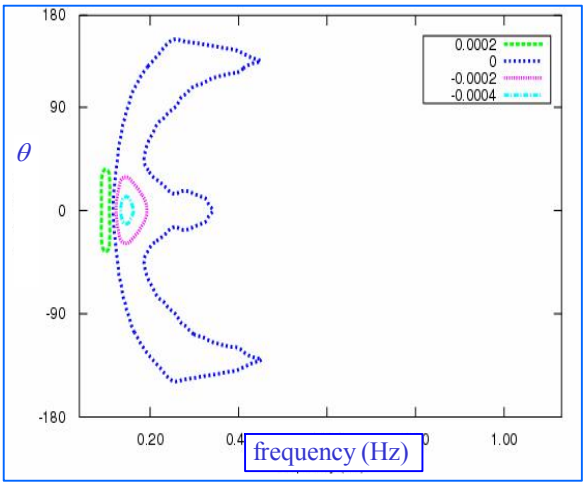

Fig. 2c. As in Fig. 2b using RTW-ww3 for S_{nl}.

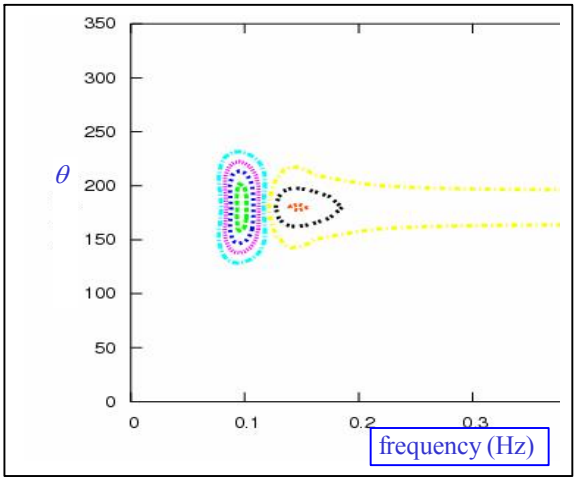

Fig. 2d. As in Fig. 2b using RTW-erdc for S_{nl}.

As a further examination of nonlinear transfers from these formulations, Figs. 3a-3d consider a highly sheared spectrum composed of two single peaks, one with f_p=0.1, $\alpha = 0.01$, $\gamma = 1$ and mean direction $\bar{\theta}$ at 180°, and the second superimposed peak with f_p=0.15, $\alpha = 0.01$, $\gamma = 3$ and mean direction $\bar{\theta} = 90°$. The input wave spectrum is given in Fig. 3a. Significant degradation is evident in results from DIA or RTW-ww3, in Figs. 3b-3c, in terms of S_{nl} magnitude, relative to results for the revised RTW-erdc version in Fig. 3d. Moreover, although the spectrum is highly sheared, it is still evident that significant nonlinear transfers to the equilibrium range occur in the RTW-erdc formulation, but not in either the DIA or the RTW-ww3 versions, as also found in Fig. 2d. We suggest that this results from the spectral tail imposed on the WW3 parameterization.

Fig. 3a. Sheared double-peaked input energy spectrum

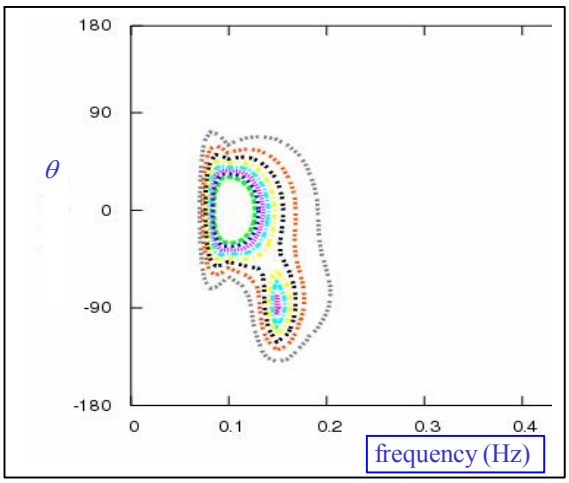

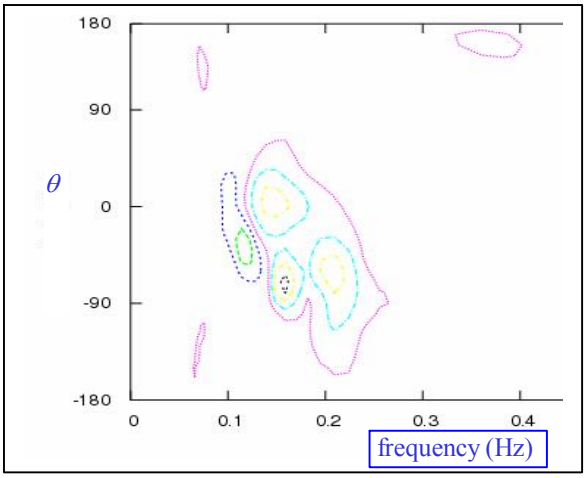

Fig. 3b. Nonlinear transfers S_{nl} for sheared spectrum $E(f,\theta)$ in Fig. 3a, using DIA from WW3.

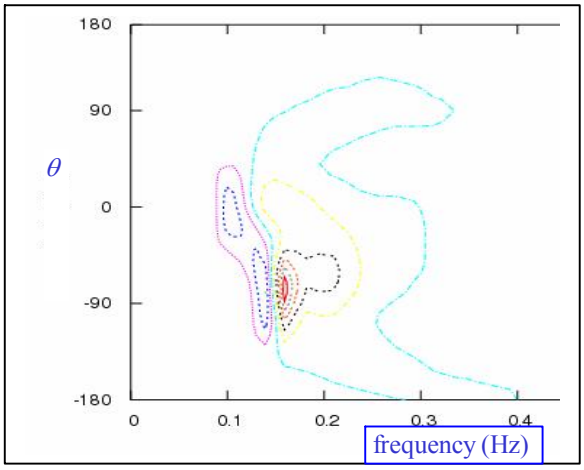

Fig. 3c. As in Fig. 3b using RTW-ww3 for S_{nl}.

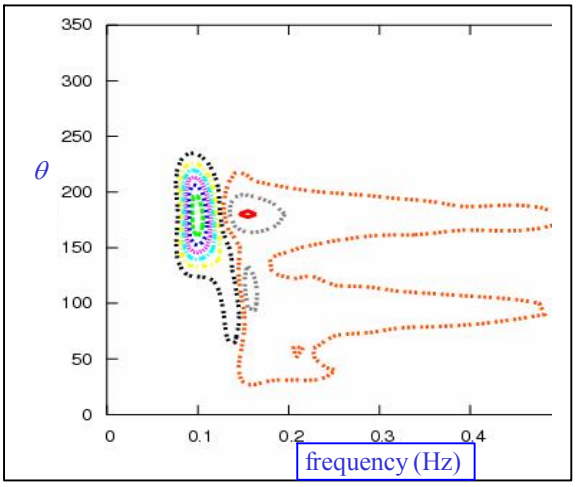

Fig. 3d. As in Fig. 3c using RTW-erdc for S_{nl}

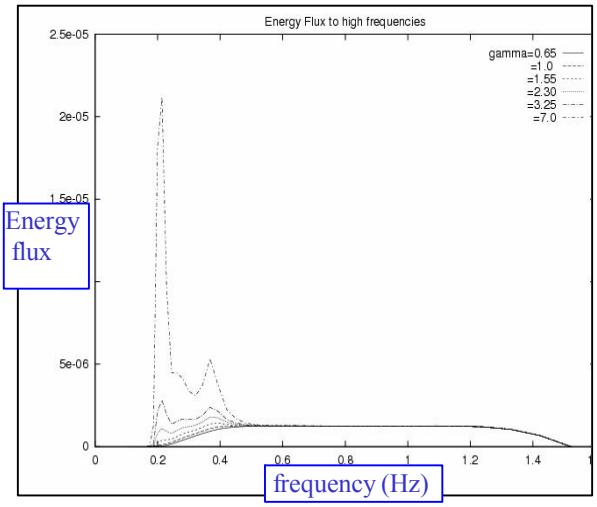

Fig. 4a. Energy flux from high to low frequencies, as a function of wave maturity –peakedness (gamma, γ).

3. ENERGY FLUXES

A measure of the primary role of nonlinear interactions within the wave spectrum is given by the energy fluxes within the spectrum. This includes both direct and inverse energy fluxes. For the DIA and RTW formulations, we evaluate the location of the "null point" f_o, in terms of conventional wave spectral parameters. This location is where no net energy is transferred via wave-wave interactions (i.e. a point where the direct and inverse fluxes are equal). Thus at f_o, there is no net transfer of energy to high frequencies, where it is lost due to dissipation. Moreover, the net input energy for frequencies below f_o, including the spectral peak region and the spectral forward face (minus whatever wave dissipative mechanisms are operative below f_o) is effectively the net energy retained by the wave spectrum. This is because no net flux occurs across f_o, in particular to the high frequency region of the spectrum where dissipation dominates over the other processes. Thus, simulation of f_o and its evolution and development is quite important, in terms of simulation of spectral development.

Figure 4a presents examples of fluxes from low to high frequencies, and Fig. 4b, fluxes from high to low frequencies, respectively, as a functions of spectral maturity, as determined by peakedness, γ. These figures were computed from the revised RTW-erdc formulation of S_{nl}. They also give an indication that f_o is a function of wave maturity, in a similar sense as spectral peak frequency, f_p, or wave age cp/u*, where cp is the phase velocity at f_p, and u* is the friction velocity. Clearly it is important for the S_{nl} formulation to have reasonable transfers to the equilibrium range in order for f_o to behave properly, and for the dominance of direct fluxes

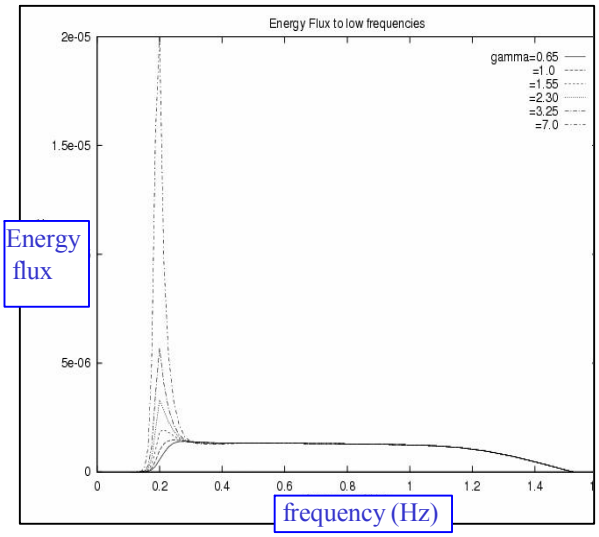

Fig. 4b. As in Fig. 4a: energy flux from low to high frequencies, as a function of peakedness (gamma).

to occur in the equilibrium range, as shown in Figs. 4a-4b.

4. NULL FREQUENCY f_o VARIATION

Figure 5a presents an example of the variation of f_o with wave maturity, expressed in terms of peakedness γ, where we have presented results from both DIA and RTW-ww3 formulations for the nonlinear interactions S_{nl} (as given by the WW3 code). Analogous results are presented in Fig. 5b, as obtained from the RTW-erdc code. The differences are striking.

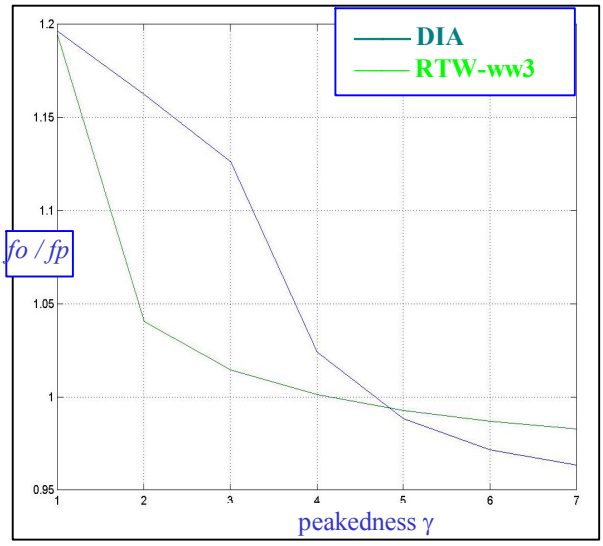

Fig. 5a. Variation of f_o(DIA)/ f_o(WRT-ww3) to spectral wave maturity – peakedness (gamma, γ).

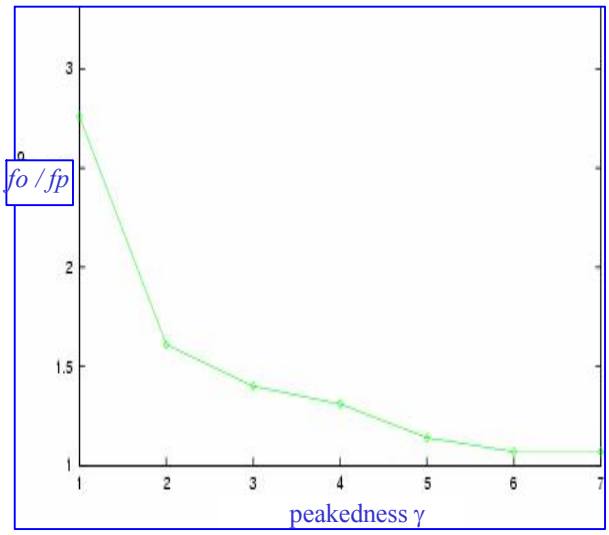

Figure 5b. As in Fig. 5a from the RTW-erdc formulation.

These results suggest biases in the WW3 version of RTW formulation of S_{nl}. In particular, it is notable that $f_o/f_p > 1$, in Fig. 5b, showing that the null frequency f_o is always above the peak f_p in the RTW-erdc results, whereas that is not the case in Fig. 5a, for either the DIA results or in the RTW-ww3 results. This means that in the case in Fig. 5b, during the young wave stages of growth, energy is being retained by the wave system, as $f_o/f_p > 1$. However, as Fig. 5a shows that this is not the case for WW3, this model is not retaining as much of the energy as it should retain, particularly from the most energetic spectral regional, around the peak f_p.

For young wave spectra, with high values of peakedness γ, Fig. 4a shows that the RTW-ww3 formulation of S_{nl} implies that although initially $f_o/f_p < 1$, this changes to *positive* as the waves become older. Moreover, in the DIA code, the inequality $f_o/f_p < 1$ is even more strongly evident. By comparison, we always find that $f_o/f_p > 1$, for the new RTW-erdc S_{nl} version.

As the wave spectrum matures and peakedness γ decreases, denoted by $\gamma \Rightarrow 1$, we find that $f_o/f_p \Rightarrow 1.2$, for both DIA and RTW-ww3 formulations. Moreover, the DIA version of S_{nl} gives values for f_o/f_p that increase more rapidly, than either RTW-ww3 or RTW-erdc versions, particularly when $2< \gamma <3$. However, it is notable that in magnitude RTW-erdc is considerably larger that either DIA or RTW-ww3 values for f_o/f_p, for this stage when $2< \gamma <3$ of wave maturity.

As another presentation of the results in Fig. 5a, we plot the ratios r_{DIA} / r_{RTW}, where $r_{DIA} = f_o/f_p$(DIA) from WW3 and $r_{RTW} = f_o/f_p$(RTW-ww3), as a function of spectral maturity, γ, in Fig 5c. This shows that when waves are very young with high γ, then f_o/f_p(DIA) is low compared to relative to f_o/f_p(RTW-ww3), as shown in Fig. 5a. For more mature spectra, when $2 < \gamma <3$, then f_o/f_p(DIA) is high relative to f_o/f_p(RTW) – WW3.

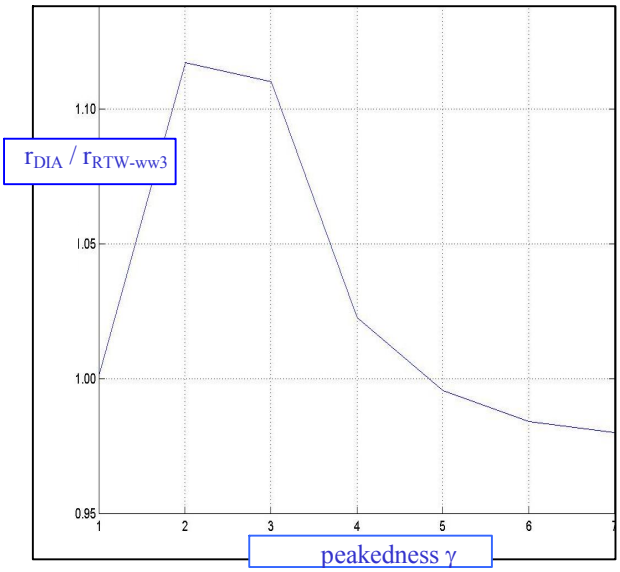

Fig. 5c. As in Fig. 5a, for the ratios $r_{DIA} / r_{RTW-ww3}$, where $r_{DIA} = f_o/f_p$(DIA) and $r_{RTW-ww3} = f_o/f_p$(RTW-ww3), as a function of spectral maturity, γ. From WW3.

5. DETAILED BALANCE

Resio et al. (2004) discuss the balance of direct (positive) and inverse (negative) fluxes within the equilibrium range beginning at about 2.5 f_p, and extending essentially to the end of the integration range, for practical

computational purposes. Throughout this range the direct fluxes are much larger than the inverse fluxes, as implicit in Figs. 4a-4b, with a dominant nonlinear transfer of energy from lower to high frequencies. For six carefully analyzed sets of field experiment data (their Fig. 3), they show normalized spectra obeying $k^{-3/2}$ behavior (or f^{-4} in terms of frequency). They note that (a) although energy flux depends on the cube of spectral density, it would not take a large deviation from $k^{-5/2}$ to accommodate net input or loss of energy due to wind input or wave breaking dissipation, and (b) within the theoretical context, their data indicate that net energy gains or losses are not so strong that they require large flux divergences to compensate for them.

Figure 6 presents evaluation of normalized energy $E(f) / f^4\beta$, as a function of f/f_p, where β corresponds to an appropriate normalization function for energies in the equilibrium range, following Resio et al. (2004).

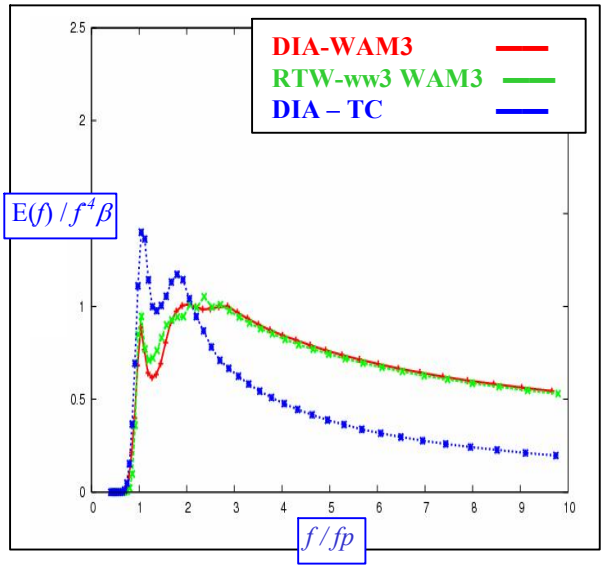

Fig. 6a. Normalized energy $E(f) / f^4\beta$, as a function of f/f_p, where: (a) DIA-WAM3 uses the DIA version of S_{nl} and the WAM3 formulations for wind input S_{in} and wave dissipation S_{ds}, compared to (b) RTW-ww3 version of S_{nl} + WAM3 Sin and S_{ds}, and (c) DIA version of S_{nl} + Tolman and Chalicov (1996) version of S_{in} and S_{ds}. After 5 hours simulation time.

This figure shows that there is no distinctive equilibrium range using DIA for $S_{nl,}$ with the Tolman and Chalicov (1996) Tolman (2002) source terms S_{in} and S_{ds}.

By contrast, given an appropriate normalization factor β, both (a) the DIA version of S_{nl} and the WAM3 (WAMDI, 1988) formulations for wind input S_{in} and wave dissipation S_{ds}, and (b) the RTW-ww3 version of S_{nl} + WAM3 Sin and S_{ds}, are able to achieve a limited approximation of an equilibrium range which can be compared to the data from Resio et al. (2004)'s Fig. 3. After 30-hours integration, as shown in Fig. 6b, there is evidence of an equilibrium range for the simulation using the DIA version of $S_{nl,}$ with Tolman and Chalicov (1996)'s S_{in} and S_{ds}, although it is shifted relatively close to the spectral peak f_p, compared to the other two test simulations, or to the data of Resio et al. (2004).

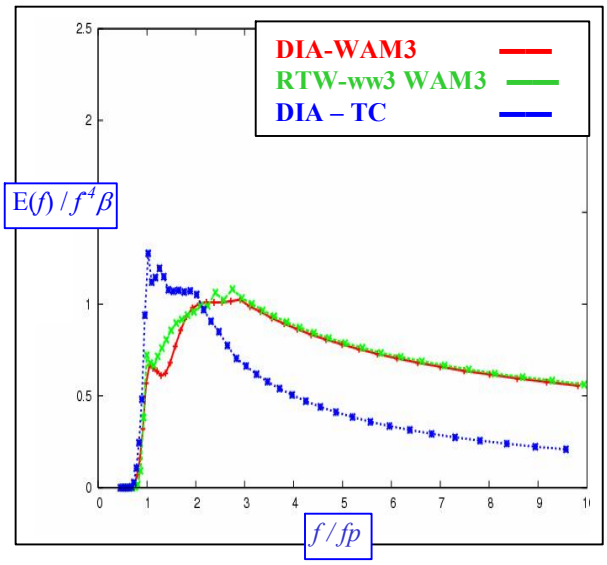

Fig. 6b. As in Fig. 6a after 30-h integration time.

In all three cases, particularly in Fig. 6a after 5-hours integraton time, the models exhibit minima between the spectral peak regions, and their equilibrium ranges, at about 1.3-1.4 f_p, which is not apparent in any of the data from Resio et al. (2004). As shown in Fig. 6b, this is also evident in the results using the Tolman-Chalicov version for S_{in} and S_{ds}, after 30-hours simulation, although the effect is less notable.

There is no indication of this feature (local minima between the spectral peak region and the equilibrium range) in computations using RTW-erdc, in conjunction with JONSWAP – type input spectra, as shown in Fig. 6c. These experiments were repeated for a variety of parameters to represent developing and maturing sea conditions. Moreover, in time-limited duration experiments it is necessary to modify standard WAM3 formulations for input energy S_{in} and wave-dissipation S_{ds} quite significantly in order to achieve the same type of peak – to-equilibrium range behavior as shown in Fig. 6c. Specifically, to achieve the peak – to – equilibrium range behavior seen in Fig. 6c, example experiments could (a) decrease S_{in} by a factor of 10, or (b) increase S_{ds} by a similar factor of 10. This is shown in Fig. 6d.

However, radical modifications to WAM3 versions of S_{in} and S_{ds} shown in Fig. 6d are not consistent with

accepted fetch-growth rules for total energy (Section 7).

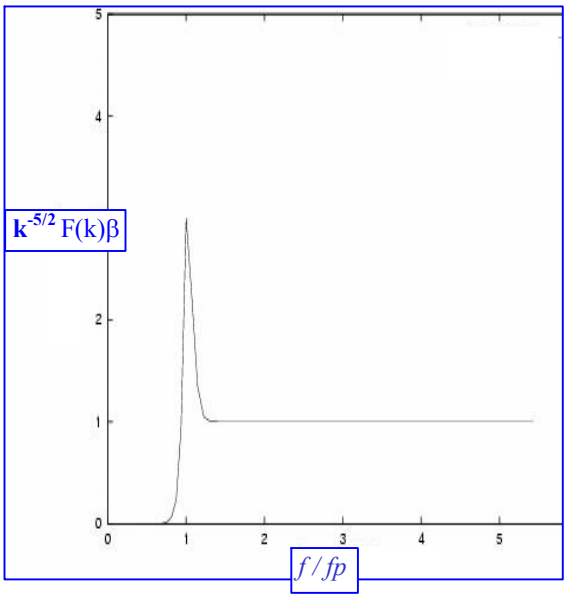

Fig. 6c. Normalized F(k) as a function of frequency, assuming a JONSWAP-type spectrum with usual parameters α= 0.01, U_{10}=15ms^{-1}, f_p= 0.1, γ=3, σ_A=0.07, σ_B=0.09, cosine spreading exponent, n=4.

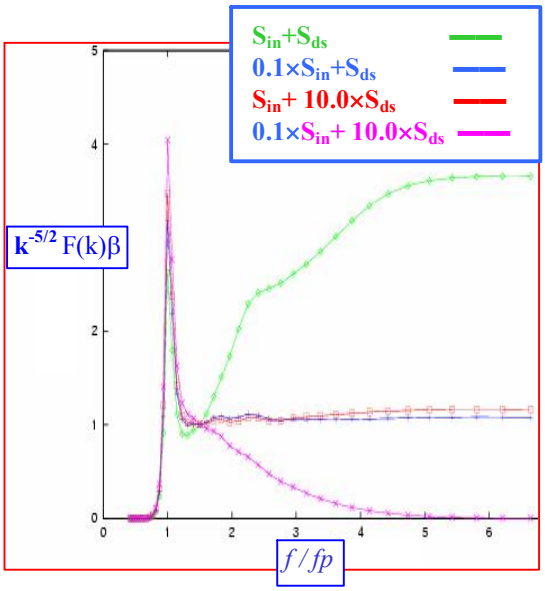

Fig. 6d. As in Figs. 6a-6b, with RTW-erdc for S_{nl}, and WAM3 versions of S_{in} and S_{ds}, and 1-hr simulation.

6. EQUILIBRUM RANGE COEFFICIENTS

One would expect that given the differences noted in f_o as estimated by the DIA formulation of S_{nl}, compared to the RTW formulations of S_{nl}, resultant differences in detailed balance within the spectrum would also be large.

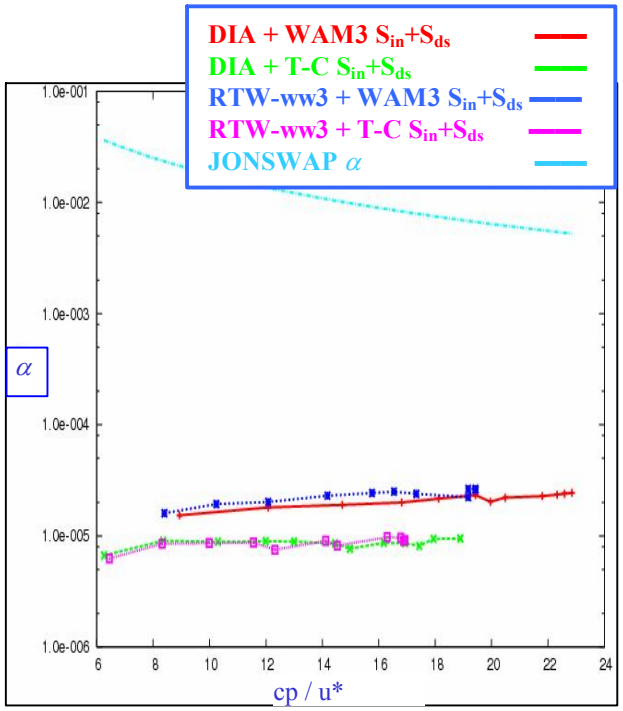

Figure 7: Variation of alpha (α) as a function of wave age cp, using both WAM3 as well as Tolman – Chalicov (denoted T-C) versions of S_{in} and S_{ds}, and also, DIA and RTW-ww3 formulations for S_{nl}, in comparison with JONSWAP's α (Eq. 2.82, Komen et al., 1994).

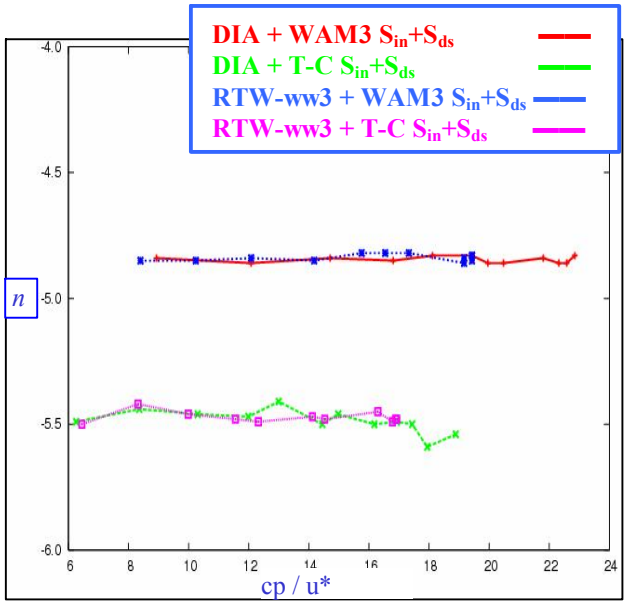

Figure 8. As in Fig. 6 for the variation of "n" – the high frequency dependency f^n. .

We completed preliminary comparison tests using wind input S_{in} and wave-dissipation S_{ds} source terms

from WAM3 (WAMDI, 1988) as well as new versions from Tolman and Chalicov (1996), and Tolman (2002). Figures 7 and 8 give results for Phillips' α coefficient and equilibrium range exponent "n", where f^n is the high variation in the spectral tail, in terms of frequency.

In Fig. 7, we find that all model simulations differ from the JONSWAP α relation, (Eqn 2.82 Komen et al. 1994),

$$\alpha = 0.57\ (cp / u^*)^{-3/2} \qquad (1)$$

and from the Resio et al. (2004) data sets, suggesting a high wave number variation $k^{-5/2}$ or f^4.

These figures show the almost complete dominance of these WAM3 and T-C formulations for S_{in} and S_{ds} source terms, over S_{nl} in WW3 wave model, *and* the effect of the high frequency parametric spectral tail. For example, if we use WAM3 formulations for S_{in} and S_{ds}, with either DIA or RTW-ww3 formulations for S_{nl} then α ~ 1.6E-4 and n ~ -4.7. On the other hand, if we use Tolman-Chalicov formulations for S_{in} and S_{ds}, with either DIA or RTW-ww3 formulations for S_{nl}, then α ~ ~1.0E-5and n ~ -5.5.

7. PARAMETRIC BALANCE

An important issue in wave modeling, besides the inability of DIA to represent the characteristics of nonlinear transfers for a specific spectrum, is the question of how DIA performs in calculations of wave growth over time and fetch. This can be termed as 'parametric balance' because wave growth rules represent parameterizations from carefully conducted field experiments. JONSWAP relations represent a prime example, of parametric fetch-growth relations.

Figures 9-10 present the fetch-limited and duration – limited results for simulations used in this study, compared to results with the JONSWAP curve. A number of observations are immediate. For example, all fetch-limited simulations, as well as all duration-limited growth curves appear somewhat too shallow in slope compared to the corresponding JONSWAP curves.

Moreover, for either fetch-limited growth, or duration-limited growth, there are clearly two families of curves: one for simulations using WAM3 S_{in} and S_{ds} source terms, and another for simulations using Tolman – Chalicov versions for S_{in} and S_{ds} source terms. For the fetch-limited growth curves, the WAM S_{in} and S_{ds} source terms appear to give a better match to the JONSWAP curve, than the Tolman-Chalicov S_{in} and S_{ds} source terms. This conclusion is not clear for the duration-limited growth curves: comparison with JONSWAP does not appear to favor one set of sources more than the other.

Moreover, for either fetch-limited growth, or duration-limited growth, the WAM S_{in} and S_{ds} source appear to result in less variation in growth – curve slope as a function of wave age (variation with time or space point), than the corresponding Tolman –Chalicov source terms, particularly for very young waves. Finally, as implemented within the Wavewatch III formulation there does not appear to be notable difference between results using WAM3 S_{in} and S_{ds} source terms in conjunction with (a) DIA or in conjunction with (b) RTW-ww3, as a representation of S_{nl}. Results from simulations using either set of source terms appear to give results that are quite similar.

Figure 10 also includes a simulation using a single – point version of the RTW-erdc version of S_{nl} in conjunction with WAM3 source terms for S_{in} and S_{ds}. This simulation appears biased quite high relative to all other simulations. Moreover, while the WAM3 source terms clearly need to be scaled down in order to match magnitudes consistent with JONSWAP observations, the rate of wave grow, as represented by the slope of the RTW-erdc curve in Fig. 10, appears to match the JONSWAP growth-curve more favorably than the other simulations displayed.

8. CONCLUSIONS

We compared DIA (WAMDI, 1988) and RTW (Resio – Tracy –Webb) S_{nl} formulations. We include the RTW-ww3 formulation within WW3, in comparison to a new revised RTW-erdc formulation. As is well known, because DIA has a very limited (two) set of discrete interactions, compared to the vast combinations of interactions available to the RTW formulations, DIA distorts the 2-dimensional energy spectrum $E(f,\theta)$ compared to RTW. An additional limitation in any operational wave forecast model is the need to impose a high frequency parametric 'tail' on the S_{nl} calculation.

These factors have impact on the ability of DIA to represent the nonlinear transfers S_{nl} compared to more 'exact' formulations such as RTW. This was explored in this paper, in terms of a simple wave spectrum compared to a two-peaked sheared spectrum. It was suggested that high-frequency nonlinear transfers were absent and lower frequency features were distorted, in comparison to a more accurate computation using the revised RTW-erdc formulation.

We considered the impacts of S_{nl} on fluxes in the high frequency equilibrium range of the spectrum. The parametric tail imposed in WaveWatchII has impact on the behavior of the 'null' frequency f_o, which is the point where the flux of action density or energy density from high to low frequencies is in balance with the flux from low to high frequencies. We show that DIA and RTW-ww3 formulations of S_{nl} have basic differences in

estimating f_o, as the spectrum develops. Moreover the RTW-ww3 formulation results in notably different f_o behavior from that of the new revised RTW-erdc algorithm. These differences have implications in terms of energy retained by the spectrum, as the system develops, because f_o defines the domain where net energy or action is retained by the spectrum.

In further exploration of the impacts of these representations of S_{nl}, we considered 'detailed balance' and the functional form of the equilibrium range. Observationally, since Toba (1973), a consensus has supported an f^{-4}, or in wavenumber space $k^{-5/2}$ variation. (Resio et al. 2004). In comparisons reported here we could find evidence that WAM3 and Tolman-Chalicov (S_{in} and S_{ds}) source terms can support equilibrium ranges. However, with the more accurate RTW-erdc code, it is necessary to impose large modification factors $\sim 10^{\pm 1}$ on the standard WAM3 (S_{in} and S_{ds}) source terms, in order to achieve simulations of equilibrium range consistent with observations.

A notable feature in all these simulations is the minima that appear to occur between the spectral peak area and the equilibrium range, at about $\sim 1.3\, f_p$. this feature is not clearly evident in recently analyzed data by Resio et al. (2004). Moreover, simulations using the accurate RTW-erdc code with JONSWAP – type spectra do not give any clear indication of these minima.

Additional features of 'detailed balance' are concerned with Philips α coefficient and the exponent n on the high frequency f^n variation. We showed that in the WaveWatch formulation, results for α and n are not sensitive with respect to DIA or RTW-ww3 formulations for S_{nl}. In either case WAM3 (S_{in} and S_{ds}) source terms give similar results for α and n, which differ from the results from Tolman – Chalicov (S_{in} and S_{ds}) source terms, and from expected values, such as α as given by Eqn 2.82 in Komen et al. (1994), or $n \sim 4$.

Results on the f^n variation for the high –frequency portion of the spectrum are connected to overall total energy growth of the spectrum in fetch-limited growth and duration-limited growth studies, as suggested by Resio and Perrie (1989). This is related to 'parametric balance', as considered in the last section of the paper.

All fetch-limited simulations, and all duration-limited growth curves appear too shallow in slope compared to the corresponding JONSWAP curves. There are clearly two families of curves: simulations using WAM3 S_{in} and S_{ds} source terms, and simulations using Tolman – Chalicov source terms. For either fetch-limited growth, or duration-limited growth, the WAM S_{in} and S_{ds} source appear to result in less variation in growth – curve slope as a function of wave age, than the corresponding Tolman –Chalicov source terms, particularly for very young waves. Finally, results using either DIA or RTW-ww3, as a representation of S_{nl} appear quite similar. Results using a single –point version of the RTW-erdc version of S_{nl} in conjunction with WAM3 source terms for S_{in} and S_{ds} appear biased quite high relative to all other simulations, but of comparable growth rates to JONSWAP observations.

Acknowledgements

Support for this research comes from Canadian Panel on Energy Research and Development (PERD - Offshore Environmental Factors Program), ONR (US Office of Naval Research) through GoMOOS – the Gulf of Maine Ocean Observing System, Petroleum Reseach Atlantic Canada (PRAC).

6. REFERENCES

Hasselman, S., and K. Hasselmann, 1985: Computations and parameterizations of the nonlinear energy transfer in a gravity – wave spectrum, part 1: A new method for efficient computations of the exact nonlinear transfer integral. *J. Phys. Oceanogr.* 15, 1369-1377.

Komen, G. J., L. Cavaleri, M. Donelan, K. Hasselmann, S. Hasselmann, and P. A. E. M. Janssen, 1994: *Dynamics and Modelling of Ocean* Waves. Cambridge Univ. Press, 532 pp.

Resio, D. T., C. E. Long, and C. L. Vincent, 2004: The equilibrium – range constant in wind-generated wave spectra. In press *J. Geophys. Res.*

Resio, D. T., and W. Perrie, 1989: Implications of an f^{-4} equilibrium range for wind-generated waves. *J. Phy. Oceanogr.* 19, 193-204.

Resio, D. T., and W. Perrie, 1991: A numerical study of nonlinear energy fluxes due to wave-wave interactions. Part 1. Methodology and basic results. J. Fluid Mech., 223, 603-629.

Tolman, H. L., and D. Chalikov, 1996: Source terms in a third generation wind wave model. J. Phys. Oceanogr. 26, 2497-2518.

Tolman H. L., 2002: User Manual and system documentation of WAVEWATCH-III Version 2.22. Technical Note. U.S. Depart. of Commerce.

Tracy, B. A., and D. T. Resio, 1982: Theory and calculation of the nonlinear energy transfer between sea waves in deep water. WIS Rep. 11, U.S. Army Engineer Waterways Experiment Station, 48 pp.

WAMDI group, 1988: The WAM model – a third generation ocean wave prediction model. J. Phys. Oceanogr., 18, 1775–1810.

Webb, D. J., 1978: Nonlinear transfers between sea waves. Deep-Sea Res., 25, 279-298.

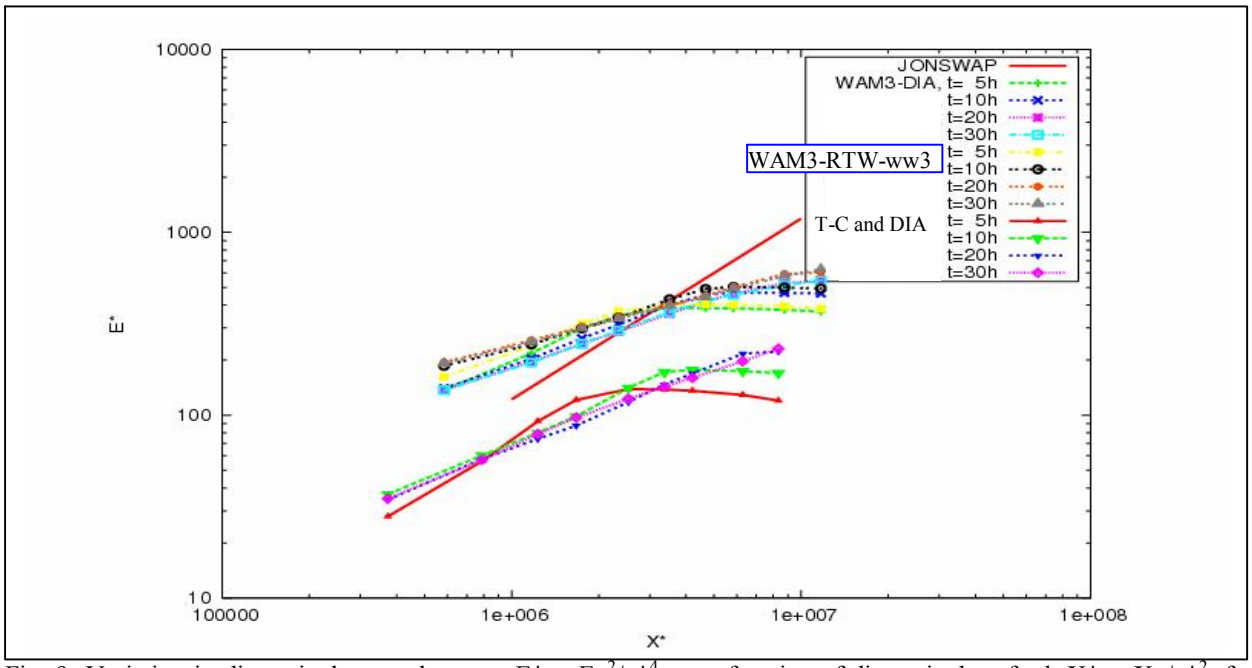

Fig. 9. Variation in dimensionless total energy $E^* = Eg^2/u^{*4}$, as a function of dimensionless fetch $X^* = Xg/u^{*2}$, for simulations using DIA and RTW-ww3 for S_{nl}, as well as WAM3 and Tolman-Chalicov for S_{in} and S_{ds}, in comparison with the JONSWAP fetch relation.

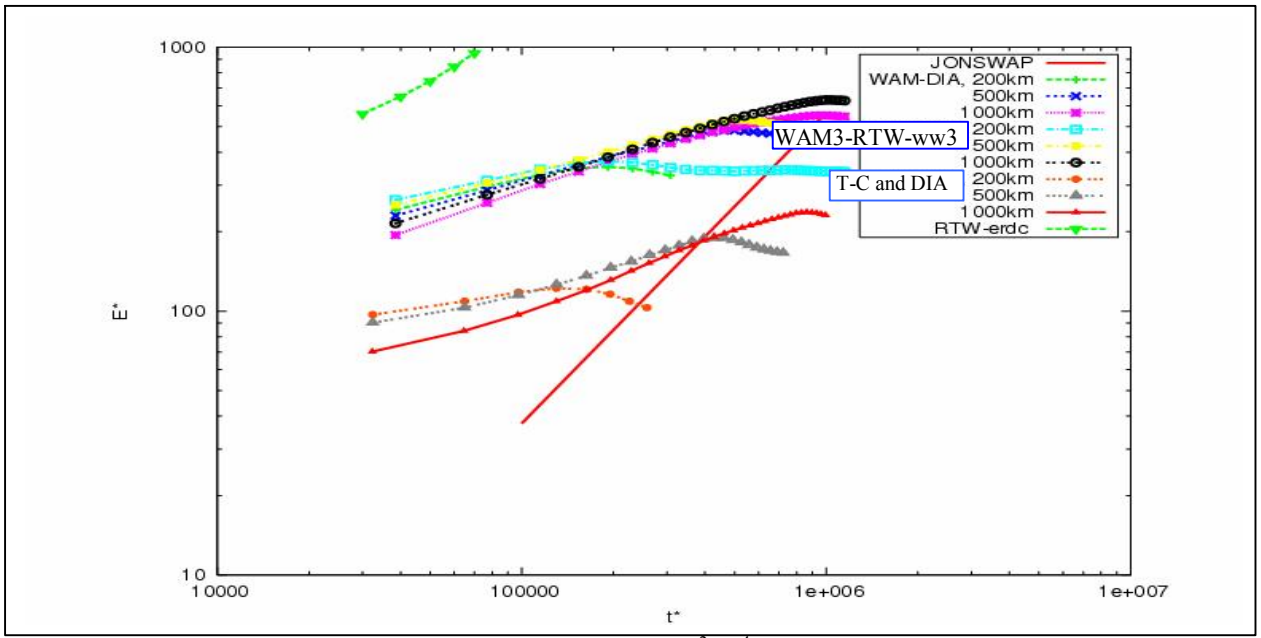

Fig. 10. As in Fig. 9, variation in dimensionless total energy $E^* = Eg^2/u^{*4}$, as a function of dimensionless time $t^* = tg/u^*$, for simulations using DIA and RTW-ww3 for S_{nl}, as well as WAM3 and Tolman-Chalicov for S_{in} and S_{ds}.